Numerical Simulation of Blood Flow Through the Aortic Arch

Berin Šeta[1], Muris Torlak[1], Alija Vila[2]

[1] University of Sarajevo, Mechanical Engeneering Faculty of Sarajevo,
Vilsonovo šetalište 9, 71000 Sarajevo, Bosina and Herzegovina
[2] K1-MET Metallurgical Competence Center, Department of Pariculate Flow Modeling, Johannes Kepler University, 4040 Linz, Austria

Abstract. Cardiovascular diseases are the most common cause of death for humans in the last decade. Understanding of the fluid flow through the aortic arch, flow properties and the influence of the blood flow on aorta's wall to make better predictions on the progress of disease. The geometric model of aortic arch is created from the series of CT scans, so that 3D model is generated. Finite-volume method is used for discretization of the equations describing blood flow. Velocity profiles, flow structure, creation of secondary and reverse flow, pressure drop on different control volumes of aortic arch are shown. Relation between the secondary flow and aortic arteriosclerosis development is confirmed. The phenomena of reverse flow in certain moment of cardiac cycle, given by the numerical simulations, coincide with theoretical and experimental results. Numerical simulations are used for better understanding and prediction of conditions triggering diseases such as aortic aneurysm and arteriosclerosis. CFD could have a significant role in detection, early prediction and treatment of the diseases.

Keywords: aortic arch, blood flow, non-Newtonian fluid, numerical simulation, computational fluid dynamics

1 Background

Cardiovascular diseases are leading cause of death of people in last decade. Some of these cardiovascular diseases affect parts of the aorta. Understanding the way how flow occurs in aorta, flow characteristics and flow impact on the wall is very important for better predictions of disease development.

One of the main reasons for numerical simulations of blood flow in aortic arch is to understand development of atherosclerosis and its impact on flow structure. It is found that early atherosclerotic lesions develop in regions where vessels branching occurs and where flow is complex in several directions. Significant disruption of the fluid flow, as previously mentioned, occurs on branches and bends of aorta as consequence of very complex geometry of aorta and pulsatile nature of blood flow. Recent studies aimed to generate physiologically relevant flow based on the real geometry and real flow conditions. Therefore, it is unacceptable to approximate the flow as stationary and geometry as theoretically ideal smooth tube.

The aortic arch is highly curved and it is expected to have skewed velocity profile with secondary flow. Also, it is expected that three leading branches to neck and brain have huge impact on flow through aortic arch.

There were many experimental and numerical studies done on simplified aorta models, like study from Yaerwood i Chandran, Barakat i Rodkievicz **[7].** These studies allowed good understanding regarding complexity of the flow through coiled pipes such as aorta. The stationary flow is determined by Reynolds and Dean number, while in the case of unsteady flow Womersleys number is involved.

2 Methodology

The Finite Volume Method (FVM) is a numerical technique that transforms the partial differential equations into discrete algebraic equations over finite volumes. Then, the system of algebraic equation is solved to compute the vales of the variables for each of the elements. FVM is inherently conservative, making it the preferred method in Computation Fluid Dynamics (CFD). Besides that, it is easy to implement boundary conditions in non-invasive manner, as unknown variables are evaluated at the center of the volume element, not at the boundary faces. In order to complete the mathematical model, initial and boundary conditions must be defined. The problem is considered well defined if the solutions exist, are unique and continuous.

2.1. Mathematical model

Mathematical model is based on the principles of continuum mechanics that are defined by conservation laws.

- *Conservation of mass*

$$\frac{\partial}{\partial t}\int_{V} \rho \, \mathrm{dV} + \int_{S} \rho \, \mathbf{u} * \mathbf{n}\, \boldsymbol{s} + \mathrm{dS} = 0 \qquad (1)$$

A. Badnjevic (ed.), *CMBEBIH 2017*,
IFMBE Proceedings 62,
DOI: 10.1007/978-981-10-4166-2_39

Where *t*is time, ρ density, dV elementary volume, *u* velocity, *n* unit vector orthogonal to the surface, *dS* elementary surface.

- *Conservation of linear momentum*

$$\frac{\partial}{\partial t}\int_V \rho\,\mathbf{u}\,\mathrm{dV} + \int_S \rho\mathbf{u} * \mathbf{u} * \mathbf{n}\,\mathrm{dS} = \int_S \sigma * \mathbf{n}\mathrm{dS} + \int_V \rho\,\mathbf{f}_\mathrm{b}\,\mathrm{dV} \quad (2)$$

Where σ is stress, $\mathbf{f}_\mathrm{b}$mass forces.

- *Conservation of energy*

$$\dot{Q} - \dot{W}_s - \dot{W}_v = \frac{\partial}{\partial t}\left[\int_V \left(\hat{u} + \frac{1}{2}u^2 + gz\right)\rho\, dV\right] + \int_S \left(\hat{h} + \frac{1}{2}u^2 + gz\right)\rho\,(u * n)dS \quad (3)$$

Where $\dot{W}_s$ is work due to shear forces, h enthalpy, $\dot{W}_v$work due to viscosity.

2.2 Discretization

Spatial discretization

Spatial domain is divided into discrete non-overlapping cells. This geometric discretization of the physical domain results in a mesh on which the conservation equation are solved. Elements are bounded by faces, that are shared between neighboring elements, except at the boundaries.

Temporal discretization

For transient simulations, governing equation are discretized in time, so the time interval is divided into certain number of time steps Δt. Problems solved in CFD are unsteady and as such require solutions where variables change as a functions of time. Every term in equations is integrated over this time step. Time integral of a given variable is equal to a weighted average between current and future values

Equation discretization

The equation discretization is performed over each element of computational domain to obtain an algebraic correlation that relates the value to values neighboring elements Surface and volume integrals are approximated by the midpoint rule, that is of 2nd order of accuracy.

Values in the faces can be obtained with interpolation, where for approximation of convective term upwind scheme is used. For approximation of other terms, most often linear interpolation is used, There are several methods for gradient approximation, such as Gauss algorithm and least square method.

3 Physiology of blood flow

Blood is a complex *mixture* of plasma (the liquid component), white *blood* cells, red *blood* cells, and platelets. Red blood cells (erythrocytes) usually take 40% of blood volume. Since erythrocytes are semi-solid particles they increase the viscosity of the blood and affect the behavior of blood. The blood is approximately four times more viscous than water. Blood does not show a constant viscosity at all flow rates, and specifically shows a non-Newtonian viscosity in micro circular systems. The non-Newtonian behavior of the blood is most evident through the small capillaries, where viscous forces dominate. However, in the most arteries blood behaves as Newtonian fluid and the viscosity may be taken as constant, 3-4cP. **[12]**

The flow rates and pressure levels are unsteady. The cyclical nature of the heart creates pulsating conditions in all arteries. Heart is released and filled with blood in subcycles systolic and diastolic. Blood is pumped from the heart during systole, while heart is resting during diastole

Fig. 1. Theoretical example of blood flow through aorta in phase of accelerating during systole (A), in phase of decelerating during systole (B), during diastole (C) (Copy from Kilner, P., et al. Circulation, 88 (5), 1993)

and does not pump blood. Aorta as the largest artery which carries the blood from the heart and serves as a repository of high pressure during cardiac cycle.

For decades, there were ongoing investigations of the flow through heart and arteries. Dean (1928) was the first who assumed that blood flow through aorta is helical flow through curved pipe. Doby and Lowman (1961) used radiopaque streamer technique to detect blood flow rotation in vivo. First studies on blood flow through aortic arch were conducted in 1970s by Seed and Wood. Those studies showed flat velocity profiles and helical flow through aorta. Studies published by Segedal and Matre showed bi-directional flow in ascending aorta from late systole to medium diastole. Blood had clockwise rotation when observed from left anterior position. [**13**] (Fig. 1.).

3.1 Basic presumptions of fluid mechanics of blood flow through the aorta

The existence of unsteady flow through the cardiovascular system includes the value if the local acceleration in most analyses. Typical Reynolds number which describe blood flow motion vary from 1 in the smallest capillaries to 4000 in the largest artery, aorta. [**10,12**]. Thus, there are differences between flow rates where inertial forces are dominant (arteries) and those flows where viscous forces are more dominant (capillaries and veins). Dimensional analysis of non-stationary Navier-Stokes equations as result give dimensionless number labelled as Womersley parameter:

$$Wo = R\sqrt{\omega/v} \tag{4}$$

Where R denominates radius of the tube, ω is angular frequency and v is kinematic viscosity.

Womersleys parameter can also be characterized as the ratio of non-stationary forces and viscous forces. When Womersley number is small, viscous forces dominate, velocity profiles are parabolic and medium speed line oscillate in phase with the pressure gradient. For Womersley numbers above 10, non-stationary inertial forces dominate the flow and velocity profile is flat. Unsteadiness of the flow cannot be ignored and there are certain characteristics of blood flow through aorta which can be seen as less important to flow nature. These characteristics are elasticity of the walls, the non-Newtonian viscosity, semi-liquid matter in the fluid, body forces and temperature. Although each of these characteristics influence the flow, flow analysis is considerably simplified if these characteristics are neglected, as it is case in the most of studies on artery flows.

3.2 Entrance region into aorta

The flow in the entrance of aorta is not fully developed. Velocity profile is flat and as flow develops midline velocity increases, while velocity near the wall decrease. Unsteady flow in the inlet region depends on Womersley and Reynolds number. If Womersley number is small, length required for fully developed flow primarily depends on Reynolds number and maximum length required for flow development is same as in stable flow under highest flow rates. For Womersley numbers bigger than 12.5 development of boundary regions is faster and almost equivalent to the length of flow development in stationary case. Aortic arch, examined in this paper is the three-dimensional helical tube which is rotated by more than 180°. Apart from the current underdevelopment that characterizes the root of the aorta, it is characteristic that fluid core in the bend with potential vortex is tilted toward the inner wall. For other arteries except aorta the flow is always tilted to outer wall.

4 Problem description

In this section of the paper were carried out tests of flow through aortic arch. Special attention was paid to the appearance of velocity profiles and pressure drop through aorta. In addition to primary flow, vortex was examined which represent secondary flow. Certain approximations were made to simplify the problem:

- The walls are rigid,
- The walls are smooth,
- The flow is in some simulation was specifically developed,
- The temperature is constant,
- The geometry of aorta is manually refined in places with atypical surface.

Other flow characteristics taken into account:

- Non-Newtonian fluid,
- Unsteady flow,
- Pulsating flow,
- The real geometry,
- Laminar or transitional flow,
- Three-dimensional flow.

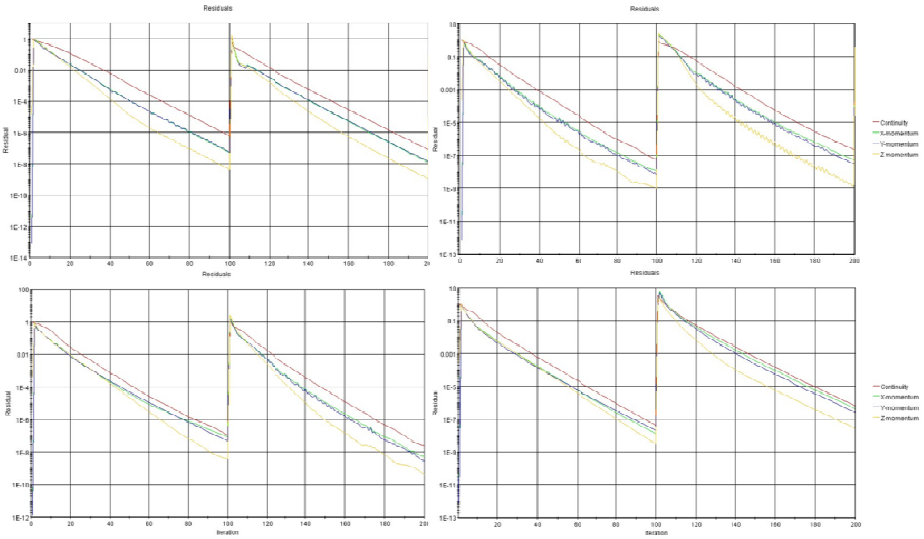

Fig. 2. Residuals under four different time steps and with hundred inner iterations

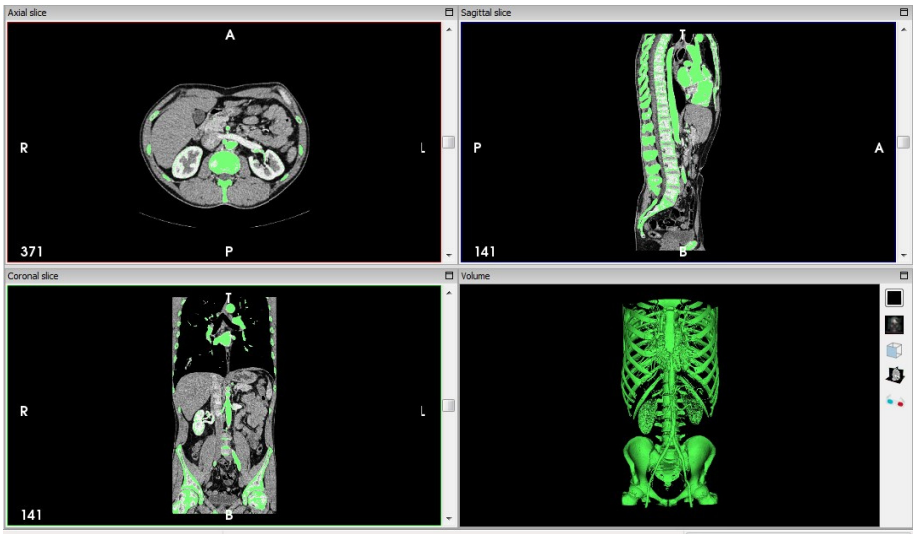

Fig. 3. Display of the 2D images (up left, up right and down left) and generated 3D model (down right) in software InVesalius

Simulations were carried out with 4 different time steps and 100 internal iterations (Fig. 2.). Since the objective was to obtain residuals in order of e-4, different steps were tested. Those time steps were 0.0075s, 0.01s, 0.02s, 0.04s. Number of 100 internal iterations was taken because of assumption that residual will converge significantly under order of e-4, and to thereby determine the largest possible step that stable converges. Two steps were simulated for those four values of time step. It is important to note that the input velocity changes every 0.01s.

In the first time step greatest convergence is achieved with a time step value of 0.01s, while in the second time step, as it was expected, greatest convergence is achieved with the smallest time step value of 0.0075s. The largest residuals are with highest time step of 0.04s. The time step chosen for final model was model with 0.01s time step, since for the same physical time it is required 13.33 times less total iteration for same convergence. Selected model with the value of 0.01s time step in the first-time step converges to residual of e-4 order in 52 iterations. Based on that the anticipated number of inner iteration for sufficiently good accuracy is 50.

4.1 Geometry and mesh

Second chapter describes process of creating geometry using program InVesalius. InVesalius is medicine aimed software that is used for virtual reconstruction of human body parts. It generates 3D models of human body parts based on series of 2D pictures that can be collected using CT (computed tomography) or MRI (magnetic resonance imaging). After construction of 3D DICOM model, program allows generation of STL data (stereolithography). The program also allows manual or semi-automatic model segmentation. This way, it is possible to gather even the smallest parts of human body if CT/MRI scans are of high quality (Fig. 3.).

DICOM data processing and creating three-dimensional models consist of 4 steps:

- Loading series of 2D pictures,
- Manual or predefined marking region of interest,
- 3D model configuration,
- Exporting model in different extesion (for this research STL format is of high importance).

After geometry has been imported into Star-CCM+ it is necessary to manually refine surfaces. In order to avoid influence of individual aortas, several models (patients of both sexes and age) have been created and then averaged using surface repair option in Star CCM+.

Some samples of aorta deformation are given in Fig 4. Aorta deformations can be caused by CT and MRI scans or physical deformation of aorta in patients.

After model creation, mesh was created automatically. Models used in the mesh are:

- Polyhedral mesh with base cell size of 1mm,
- Prism layers on aorta boundaries (10 layers of total thickness 1mm),
- Surface remesher.

Total number of cells is 299237. Average radius of aorta inlet is 2.63cm and average radius of outlet to abdominal aorta is 2.05cm.

4.2 Initial and boundary conditions

The flow through the aorta is a pulsating unsteady flow, which is defined by three numbers: Reynolds, Deans and Womersleys number. Model used in the simulation is implicit unsteady model with 50 inner iterations and time step of 0.01s. Number of inner iterations and time step are selected on basis of residual convergence which on the initial testing was bellow of e-4 order. Except implicit unsteady model, laminar model is selected with constant density of 1060 kg/m^3. Blood is defined as non-Newtonian with variable viscosity. In this model Carreau-Yasuda model was used where dynamic viscosity is not dependent on the speed of deformation due to shear stress $\dot{\gamma}$.

$$\eta(\dot{\gamma}) - \eta_\infty(\eta_0 - \eta_\infty)(1 + (\lambda\dot{\gamma})^\alpha)^{\frac{n-1}{\alpha}} \quad (5)$$

where are a, n i λ denominate empirical defined values which define curve between η_∞ and η_0.

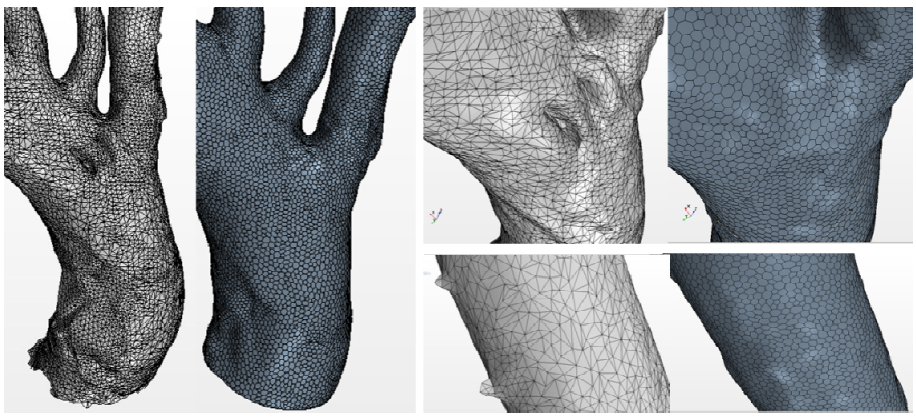

Fig. 4. Example of geometry before (images on left side) and after (images on the right side) using option surface repair

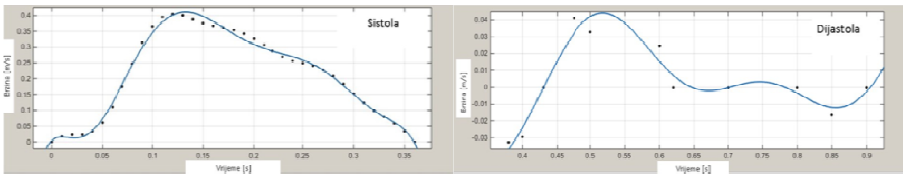

Fig. 5. Systole and diastole approximated and plotted Mathlab curve fitting

This model define three regimes:

- Newtonian region η_0 for small velocity of deformations,
- Region where η is getting lower with $\dot{\gamma}$,
- Newtonian region with constant η_∞.

In this study coefficients were taken from Boyd et. al. (2007) [**15**]. .

One cardiac cycle lasts 0.9s or 90 time steps, systole lasts 0.36s and diastole 0.54s. As input data tables of velocity values in every direction are used. Data tables are created in C++ and Matlab. Option used in Matlab is curve fitting tools, so that experimental inlet values of mass flow rate in aorta entrance are interpolated. For better overall interpolation, systole and diastole are separately interpolated.

Systole is interpolated with polinom of eight order. Function form (Fig. 5.):

$$f(x) = p_1x^8 + p_2x^7 + p_3x^6 + p_4x^5 + p_5x^4 + p_6x^3 + p_7x^2 + p_8x + p_9 \quad (6)$$

Equation used to approximate inlet during diastole is sum of three sinus equation with form of (Fig. 5.):

$$f(x) = a_1 sin(b_1x + c_1) + a_2 sin(b_2x + c_2) + a_3 sin(b_3x + c_2) \quad (7)$$

The format of the table acceptable for STAR CCM+ has a form table (x, y, z, time) and it is generated using C++ code. Columns of the table give values for space coordinates of the inlet – x, y, z. In this case the value of z is equal for all the cells. In order to STAR CCM+ recognize the right format of the table and obtain correct values from the table columns, first row must have format:

$$XYZ\ VAR1[t = T1]VAR1[t = T2]VAR1 [t = T3]\ VAR2[t = TT1]\ VAR2[t = TT2] \quad (8)$$

where VAR1 represents the velocity in z direction, VAR2 velocity in x direction (in this example equal to 0) and VAR3 velocity in y (in the example, also equal to 0).

The example of the table is given as:

$$X\ Y\ Z\ Temperature(K) \quad (9)$$
$$[t = 1s]Temperature(K)$$
$$[t = 2s]Temperature(K)$$
$$[t = 3s]1\ 2\ 3\ 300\ 400\ 500$$

The method of transfer between the values given in the table can be defined with characteristics of value interpolation. In this case consecutive linear transition of values is used. Two cases were tested: the first case with tabular input and parabolic velocity profile at inlet; the second case with tabular input and uniform velocity profile. Flow split outlet was chosen for an outlet with 10% of the flow imposed towards brachial artery, 5% to each carotid arteries, and 80% to abdominal aorta.

5 Results and discussion

Results for 4 different snapshots through the cardiac cycle are presented:

- Maximum velocity increase in systole,
- Maximum velocity decrease in systole,
- Early diastole,
- Late diastole.

The snapshots in cardiac cycle are taken for time 0.13s, 0.3s, 0.4s and 0.9s. The flow characteristics and distribution can be described theoretically. It is necessary to consider the flow in aorta in the moment of highest velocity increase in systole.

Flow through the aorta arch is distributed as shown on the Fig. 7. and it is clear that 4 out of 6 flow lines are moving in proximity to the inner wall of aorta arch, as the theory suggests. It is worth noting that significant vorticity is not detected in period.

Characteristic of the second moment where velocity decrease in systole is at its maximum is the beginning of vorticity flow, with a similar flow distribution as in the first case.

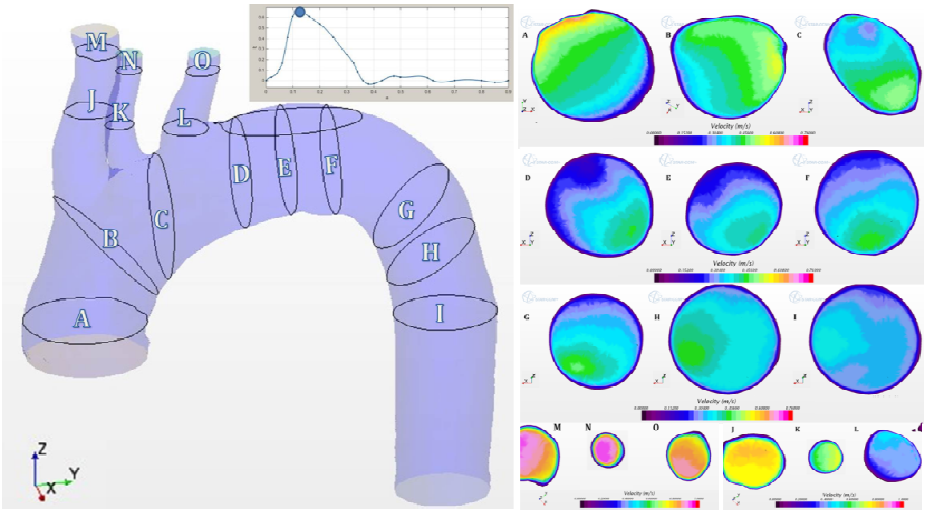

Fig. 6. Display of control volume through aorta with velocities on the peak of systole

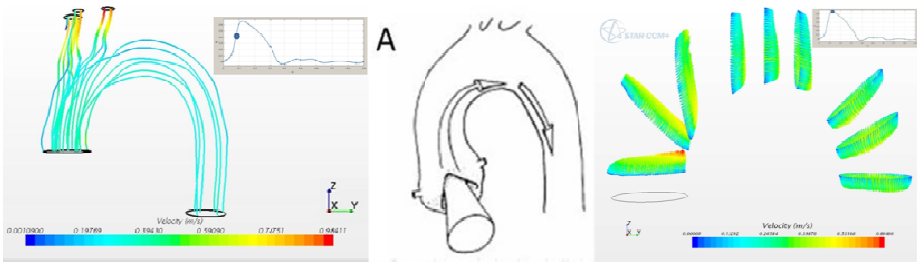

Fig. 7. Layout of the flow through aorta using stream lines in early and peak systole (numerical calculation - left; theoretical view - middle; streamlines in control volumes – right)

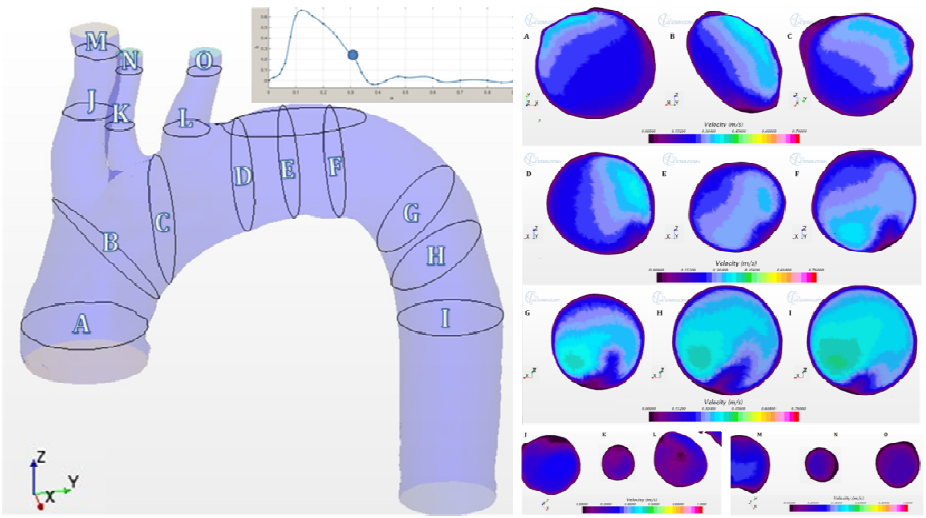

Fig. 8. Display of control volume through aorta with velocities in late systole

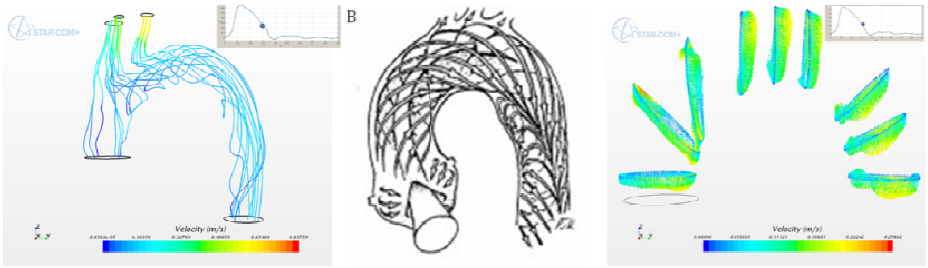

Fig. 9. Layout of the flow through aorta using stream lines in late systole (numerical calculation - left; theoretical view - middle; streamlines in control volumes – right)

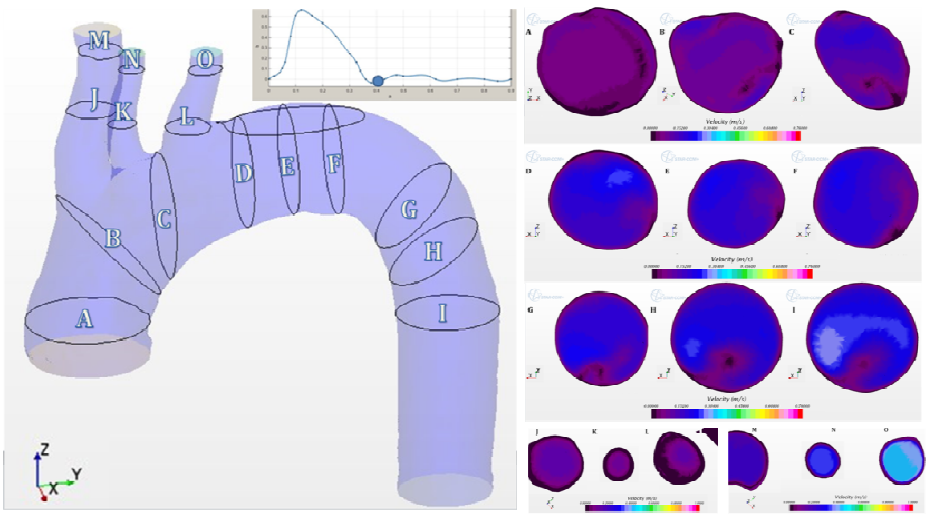

Fig. 10. Display of control volume through aorta with velocities in early diastole

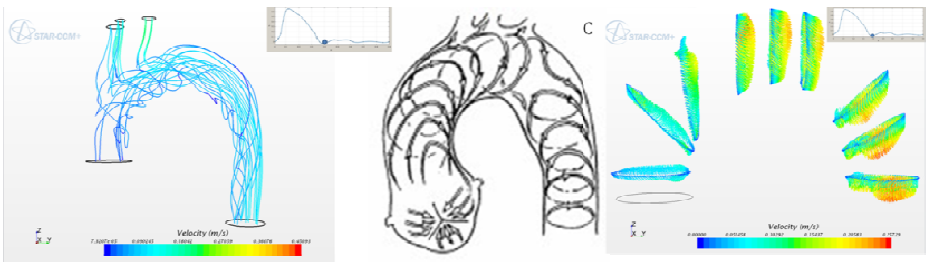

Fig. 11. Layout of the flow through aorta using stream lines in early diastole (numerical calculation - left; theoretical view - middle; streamlines in control volumes – right)

In fig. 9. theoretical solution is compared with numerical simulation. It is possible to see certain agreement in the general flow and flow lines. Second important characteristic is secondary flow that moves clockwise for the observer from front left side. Another distinguished characteristic of the last systole is the beginning of reverse flow formation at aorta branch close to the inner wall.

The reverse flow near the inner wall is also characteristic of early diastole, but not in the same order as for late systole. At this initial stage of diastole, the reverse flow through arteries that lead to neck and brain is visible and that phenomena is more visible through diastole, as it is shown in the Fig. 10..

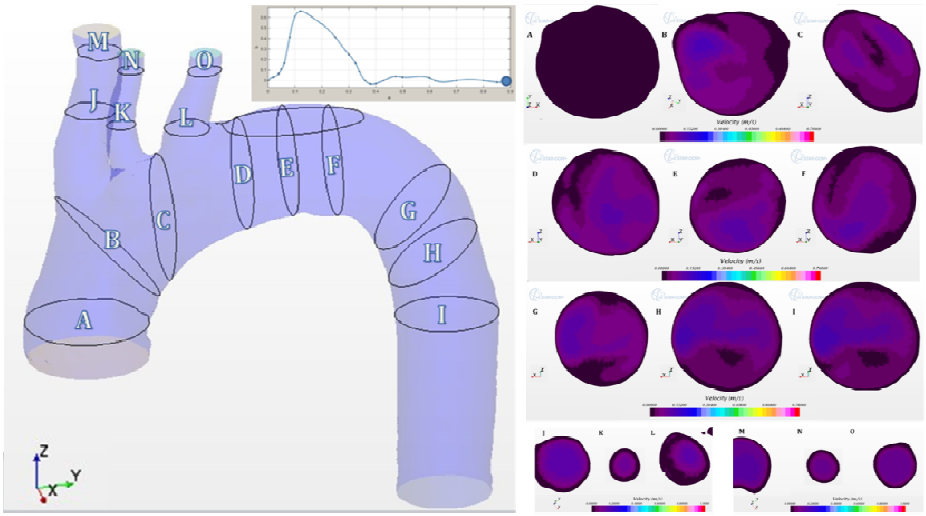

Fig. 12. Display of control volume through aorta with velocities in late diastole

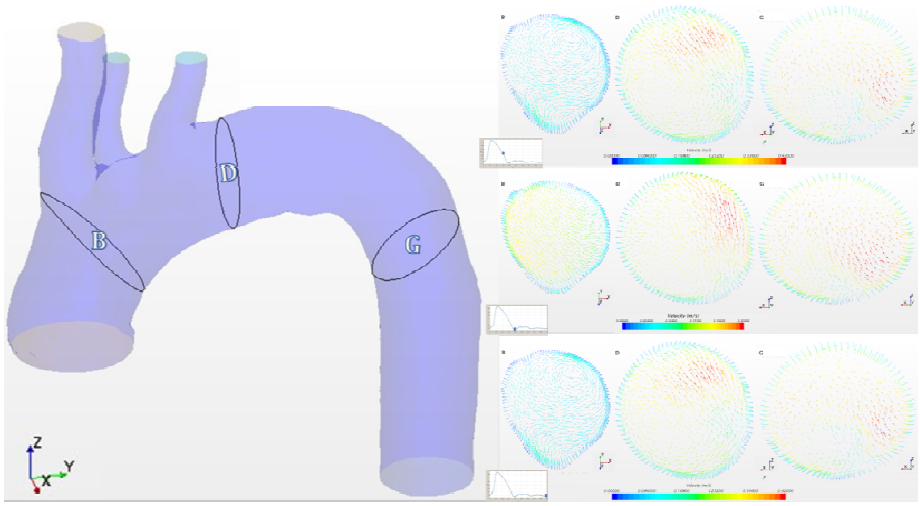

Fig. 13. Display of control volume through aorta with secondary flow

Secondary flow is pronounced through diastole and in the fig. 13 comparison between theoretical and experimental results are presented. As before, rotation is clockwise when viewed from front left position.

The forth chosen moment is immediately before the start of the systole, in order to describe the transition from diastole to systole, as well as transition of the velocity profile. Velocities are shown at 15 cross sections, while secondary flows are shown at 3 cross sections. The cases in question are for non-Newtonian Carreau-Yasuda model and flat velocity profile at the inlet.

6. Conclusion

The paper presents the flow of blood through the aortic arch. Process of getting results consisted of several steps: importing DICOM images and creating realistic three dimensional model, setting initial and boundary conditions, calculations and result analysis. On the basis of certain approximation that have been made, such as during a heart cycle of 0.9s, 0.36 during systole and 0.54s during diastole, the walls are smooth and rigid, temperature has been ignored. Such results can not accurately give results in num-

bers but can provide guidance for further work in this field. Experimental hypothesis are confirmed concerning ways and the distribution of blood flow through the arch.

Further work in this field would introduce the interaction of the fluid and the wall (as elastic) for better understanding and better prognosis of conditions such as aortic aneurysm and aortic stenosis. The elasticity of the walls in these places is not the same as in healthy aorta or in other parts of the aorta. In the case of narrowing of arterial walls, speed is increasing and turbulence can occur, while in case of aneurysm wall may break if the wall is too spread out. CFD could have a significant role in detection, early predicting and treatment of diseases.

References

[1] White, M.F.: Fluid mechanics. Seventh edition. McGraw-Hill Publishing Co. Columbus (2011)
[2] White, M.F.: Fluid mechanics. Fourth edition. McGraw-Hill Publishing Co. Columbus (1998)
[3] Xiaofeng, G., Martonen, T.B.: Simulation of flow in curved tubes. Aerosol Science and Technology. 26:6, 484-504 (1997)
[4] Toro, E.F.: Riemann Solvers and Numerical Methods for Fluid Dynamics, Springer-Verlag, Berlin Heidelberg New York (2009)
[5] Ferziger, J.H., Peric, M.: Computational Methods for Fluid Dynamics. Third edition. Springer-Verlag, Berlin Heidelberg New York (2002)
[6] Nicols, W.W., O'Rourke, F.M., Vlachopoulos, C.: McDonald's Blood Flow in Arteries- theoretical, experimental and clinical principles. Sixth edition. Hodder Arnold (2011)
[7] Shahcheraghi, N., Dwyer, H.A., Cheer, A.I., Barakat, T.R.: Unsteady and Three-Dimensional Simulation of Blood Flow in the Human Aortic Arch. J Biomech Eng. 124, (4), 378-387 (2002)
[8] Kenjeres, S.: Modeling and simulation of multy-physics multi-scale transport phenomenain bio-medical applications. XXI Fluid Mechanics Conference. Journal of Physics: Conference Series 530 (2014)
[9] Chares, A.T., Draney, T.M.,: Experimental and Computational Methods in Cardiovascular Fluid Mechanics. Annu. Rev. Fluid Mech. 34: 197-231 (2004)
[10] Van de Vosse, N.F., Stergiopoulos, N.: Pulse Wave Propagation in the Arterial Tree. Annu. Rev. Fluid Mech. 43: 467-499 (2011)
[11] Kenjeres, S., de Loor, S.: Modelling and simulation of low-density lipoprotein transport through multi-layered wall of an anatomically realistic carotid artery bifurcation. Royal Society Publishing (2013)
[12] Ku, N. D.: Blood Flow in Arteries. Annu. Rev. Fluid Mech. 29, 399-434 (1997)
[13] Suo, J.: Investigation of blood flow patterns and hemodynaics in the human ascending aorta and major trunks of right and left coronary arteries using magnetic resonance imaging and computational fluid dynamics, Doctoral disertation. Georgia Institute of Technology (2005)
[14] Demirdžić, I: Mehanika fluida. Mašinski fakultet Sarajevo, Sarajevo (1990)
[15] Boyd, J., Buick, M. J., Green, S.: Analysis of the Casson and Carreau-Yasuda non-Newtonian blood models in steady and oscillatory flows using the lattice Boltzmann method. Physics of Fluids, Vol 19. (9) (2007)